Catalysis Today 156 (2010) 118–123

Contents lists available at ScienceDirect

Catalysis Today

journal homepage: www.elsevier.com/locate/cattod

H_2O_2 synthesis over PdAu membranes

Lei Shi, Andreas Goldbach*, Gaofeng Zeng, Hengyong Xu

Dalian Institute of Chemical Physics, Chinese Academy of Science, Dalian 116023, China

ARTICLE INFO

Article history:
Available online 19 March 2010

Keywords:
Hydrogen peroxide
Direct synthesis
PdAu membrane
Hydrogen permeation
Membrane reactor

ABSTRACT

2–3 μm thick PdAu membranes have been prepared by sequential electroless plating on porous ceramic tubes followed by annealing at 823 K under H_2. Gas phase H_2 permeation rates had stabilized after 250 h annealing even though the alloy layers still remained inhomogeneous as evidenced by X-ray diffraction analyses after conclusion of all other experiments. The H_2 permeability of a $Pd_{90.5}Au_{9.5}$ membrane reached 1.2×10^{-8} mol m^{-1} s^{-1} $Pa^{-0.5}$ at 673 K. A marked discontinuity in the temperature dependence of the H_2 permeation rate at 573 K signals a change from diffusion to adsorption or desorption-limited H_2 transport through the membrane below that threshold. H_2O_2 was directly synthesized from the elements over these PdAu membranes in O_2-saturated, acidic water/ethanol mixtures while feeding H_2 through the membrane. The H_2O_2 formation rate increased from 19.5 to 97.5 mmol m^{-2} h^{-1} between 277 and 363 K in water at 300 kPa H_2 feed pressure even though the H_2O_2 selectivity decreased from 56% to 30% in parallel. H_2O_2 yield and selectivity improved both with H_2 feed pressure, however. H_2O_2 formation rate and selectivity increased also moderately with ethanol content, but the PdAu layer tended to delaminate from the ceramic support if the ethanol content was raised above 50%.

1. Introduction

H_2O_2 is employed in chemical industry and waste water treatment as environmentally benign oxidant. Commercially it is produced via the complicated and expensive anthraquinone process [1]. Direct synthesis from H_2 and O_2 over Pd-based catalysts has been long known too [1], but it has been considered too hazardous for industrial implementation so far because of the highly explosive nature of H_2/O_2 mixtures. Still this alternative production route has been widely studied in recent years, since it is potentially less expensive and avoids toxic byproducts. An intriguing direction in these studies was initiated by Choudhary et al. when they proposed the utilization of dense Pd-type membrane catalysts instead of powder catalysts to circumvent H_2/O_2 mixtures [2]. There, H_2 is dosed through the membrane into an O_2-charged solution to keep H_2 and O_2 effectively separate and overcome the safety issue (Fig. 1). The concept of feeding H_2 and O_2 from opposite sites of a diaphragm has been also studied using porous separation barriers in membrane contactor applications [3,4].

One particularly attractive implementation of the dense membrane concept could be *in situ* generation of H_2O_2 for selective oxidation in liquid phase. For example, epoxidation reactions are frequently performed above room temperature up to 363 K [5,6]. Hence, we have investigated H_2O_2 production in this temperature range employing pure Pd membranes in an aqueous reaction medium [7]. We found that H_2O_2 productivity increased significantly with temperature despite the parallel acceleration of H_2O_2 consumption processes. In addition we observed enhanced H_2O_2 selectivities at higher H_2 feed pressures, which we ascribed to inhibition of direct H_2O formation as a result of hindered O_2 dissociation due to blocking of O atom adsorption sites on the membrane surface because of increasing occupation by H atoms [7].

We investigate now the preparation and suitability of PdAu/ceramic composite membranes for this purpose, since supported PdAu powder catalysts exhibit higher H_2O_2 formation rates and selectivities than pure Pd or Au catalysts [1,8]. On the other hand, the propensity of PdAu membranes for embrittlement under H_2 decreases with increasing Au fraction because the miscibility gap in the ternary Pd–Au–H phase diagram narrows and shifts to lower temperatures in parallel [9]. In addition, the H_2 permeability of PdAu alloys remains close to that of Pd at least up to 15 at.% Au content [10]. Thus PdAu membranes appear to be better suited as bi-functional membrane catalysts for direct H_2O_2 synthesis than pure Pd membranes. Furthermore, alcohols are frequently favored as reaction medium over water for this reaction since they feature several times higher O_2 and H_2 solubility, which benefits H_2O_2 yield and selectivity [1]. Hence we have also investigated H_2O_2 synthesis over PdAu membrane catalysts in water/ethanol mixtures at elevated temperatures in the present study.

* Corresponding author at: Dalian Institute of Chemical Physics, Laboratory of Applied Catalysis, 457 Zhongshan Road, Dalian 116023, China. Tel.: +86 8437 9229; fax: +86 411 8469 1570.
E-mail address: goldbach@dicp.ac.cn (A. Goldbach).

0920-5861/$ – see front matter © 2010 Elsevier B.V. All rights reserved.
doi:10.1016/j.cattod.2010.02.038

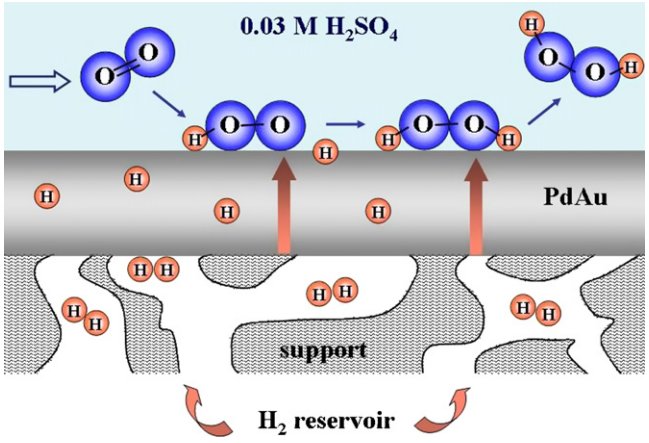

Fig. 1. Concept of liquid phase PdAu membrane reactor for direct H_2O_2 synthesis.

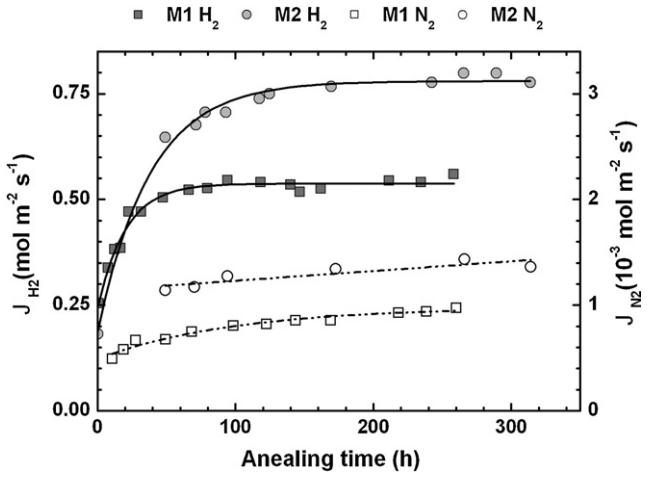

Fig. 2. H_2 and N_2 fluxes of membranes M1 and M2 during annealing at 823 K and ΔP = 100 kPa.

2. Experimental

2.1. PdAu membrane preparation and gas permeation testing

Two 5 cm long PdAu membranes were fabricated by sequential electroless plating of Pd and Au onto the outside surface of 30 cm long, porous ceramic tubes (8 mm i.d., 12 mm o.d., Nanjing University of Technology). The rest of the surface and one end of each tube were sealed airtight with a glaze. Pd deposition has been described previously [11]. Non-cyanide electroless plating of Au was carried out in a homemade Au plating solution (Table 1) at 333 K and pH 10, which has been described elsewhere in more detail [12]. The alloy composition was initially controlled by plating time and estimated by gravimetric analysis. The freshly prepared Pd/Au membranes were mounted in a gas permeation setup and heated in N_2 to 623 K before switching to H_2 and heating to 823 K for alloying. Alloy formation was monitored by measuring the H_2 permeation rate. After stabilization of the latter the single gas H_2 and N_2 permeation characteristics of the membranes were established over a wider temperature range. The permeate side was always kept at atmospheric pressure, and no sweep gas was used during those tests while the permeated gas was passed through a bubble flowmeter. All the gases used in experiments were 99.999% in purity. H_2 fluxes were corrected for defect flow contributions with the help of N_2 permeation data following the procedure outlined by Uhlhorn et al. [13].

2.2. H_2O_2 synthesis

H_2O_2 synthesis was carried out in a glass reactor that was heated in a water bath as previously described [7] using membrane M1 in ethanolic and M2 in ethanol-free reaction solutions. In short, the membrane was mounted gastight with a rubber stopper into the reactor. H_2 at 140–300 kPa was fed through the tube inside into ethanol/water mixtures containing 0.03 mol/l H_2SO_4 (Shenyang Chemical Reagent Factory), which were saturated with O_2 at atmospheric pressure through a frit at the reactor bottom and contained 5 ppm KBr. The lumen of the membrane tube and the gas line to a H_2 pressure gas tank served as a H_2 reservoir, which was cut-off from the tank after it had been charged with H_2 at a desired feed pressure P_{res}. The H_2O_2 concentration $n_{H_2O_2}$ was determined after 1 h reaction time unless otherwise stated, either by iodometric titration in alcoholic or K_2MnO_4 titration in aqueous reaction media. H_2 consumption Δn_{H_2} was determined from the pressure drop in the H_2 reservoir [7]. The composition of the gas at the reactor outlet was monitored by an on-line GC (GC-8A, Shimadzu) equipped with a molecular sieve 5A column and a TCD detector. No H_2 was detected at the outlet of the reactor by GC during experiments indicating that H_2 permeating through the membrane to the liquid reaction medium was completely consumed by reactions during H_2O_2 synthesis experiments. Thus, the H_2O_2 selectivity was determined according to Eq. (1):

$$S_{H_2O_2} = \frac{n_{H_2O_2}}{\Delta n_{H_2}}. \quad (1)$$

Table 1
Composition of Au plating bath.

Component	Quantity
$AuCl_3 \cdot HCl \cdot 4H_2O$	7.25 mM
Na_2SO_3	0.17 M
$Na_2S_2O_3 \cdot 5H_2O$	0.15 M
NaOH	0.42 M
L-$C_6H_8O_6$ (L-ascorbic acid)	0.34 M

2.3. PdAu membrane characterization

After conclusion of the H_2O_2 synthesis studies the membranes were broken and thickness and composition of the PdAu layers was determined by scanning electron microscopy (SEM, QUANTA 200F, FEI), energy-dispersive X-ray spectroscopic analysis (EDS), X-ray diffraction (XRD, Philips PANalytical, Cu Kα = 0.15406 nm at 40 mA and 40 kV) and X-ray photoelectron spectroscopy (XPS), respectively. XPS spectra were obtained with a VG ESCALAB MK2 X-ray photoelectron spectrometer using Al Kα radiation (1486.6 eV, 12.5 kV, and 250 W) as excitation source. The C 1s peak at 285.0 eV originating from carbon contaminations contracted by handling of the samples on air was used for calibration of the metal peak positions. Average XRD composition values were calculated from at least three fragments of each membrane. The Au content x_{Au} was determined from the XRD fcc lattice parameter a_0 according to a relationship taken from the literature [14]:

$$a_0 = 0.38895\,\text{nm} + (1.89 \times 10^{-4}\,\text{nm}) x_{Au}. \quad (2)$$

3. Results

3.1. Characterization of PdAu membranes

Fig. 2 displays the single gas H_2 and N_2 fluxes J_{H_2} and J_{N_2} measured during the initial alloying of the PdAu membranes at 823 K and ΔP = 100 kPa. J_{H_2} of the 2 μm thick $Pd_{87}Au_{13}$ membrane M1 increased from 0.25 to 0.47 mol m^{-2} s^{-1} within 99 h

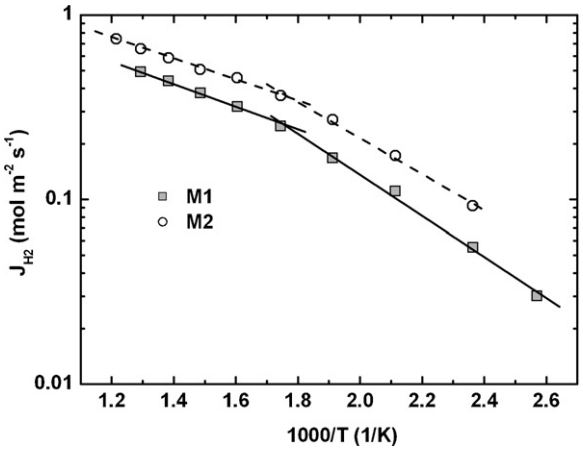

Fig. 3. Temperature dependence of H_2 flux through membranes M1 and M2 at $\Delta P_{H_2} = 100$ kPa.

and then remained at this level during the following 7 days. The stabilization of the gas phase H_2 permeation rate was taken as indication that the Pd and Au layers had been well alloyed. The N_2 leak rate of M1 increased continuously from 0.49×10^{-3} to 0.97×10^{-3} mol m^{-2} s^{-1} during this time span although its growth rate slowed down with time. After 260 h the H_2 flux was 570 times greater than the N_2 flux at 823 K. J_{H_2} of the 3 μm thick $Pd_{90.5}Au_{9.5}$ membrane M2 increased from 0.18 to 0.74 mol m^{-2} s^{-1} within 117 h and then stabilized at 0.77 mol m^{-2} s^{-1} during the following 8 days. J_{N_2} increased gradually from 1.14×10^{-3} to 1.36×10^{-3} mol m^{-2} s^{-1} resulting in an ideal H_2/N_2 selectivity of 571 after 314 h annealing.

The temperature dependence of the H_2 flux through both PdAu membranes is shown in Fig. 3. J_{H_2} increased at a much faster rate with temperature below 573 K than above. The H_2 fluxes below and above this threshold can be described by Arrhenius laws $J_{H_2} = A_0 \exp(-E_{act}/RT)$. The corresponding prefactors A_0 and activation energies E_{act} are summarized in Table 2. The pressure dependence of the H_2 fluxes deviated from Sieverts' law with pressure exponents varying around $n = 0.6$ (±0.15) in the pressure range 20 kPa ≤ ΔP_{H_2} ≤ 100 kPa.

Fig. 4 shows SEM images of the PdAu layers after conclusion of the H_2O_2 synthesis experiments. Accordingly the PdAu layer thickness of M1 and M2 were 2 and 3 μm, respectively. It can be seen that voids had formed within the alloy layers, which appear to be larger in membrane M1. Furthermore, composition analyses revealed that alloying of the Pd and Au layers had not been complete. Table 3 summarizes the PdAu layer compositions derived from XRD patterns of the top and bottom sides of membrane fragments (ca. 3 cm^2 each), from large-area, top surface EDS scans (86–64000 μm^2) and from top surface XPS scans (ca. 0.5 mm^2 fragments). XRD patterns of several fragments consistently yielded higher Au contents for the top surface than for the interface to the ceramic support (bottom surface). While the discrepancy was only around 2 at.% for the thinner membrane M1, the Au content of the M2 top surface was almost twice as high as that at the support interface. This indicates

Table 2
Arrhenius parameters of M1 and M2 gas phase H_2 permeation rates.

Membrane	T range (K)	A_0 (mol m^{-2} s^{-1})	E_{act} (kJ mol^{-1})
M1	>573 K	3.1 ± 0.1	11.7 ± 0.2
	<573 K	22.7 ± 4.8	21.2 ± 0.8
M2	>573 K	3.5 ± 0.2	10.7 ± 0.4
	<573 K	19.6 ± 4.3	18.7 ± 0.9

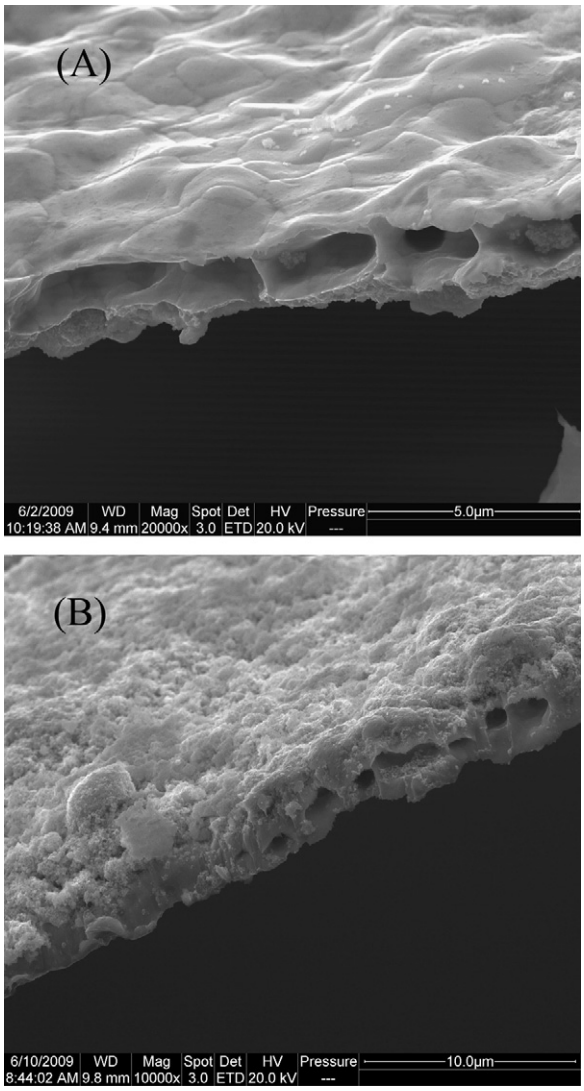

Fig. 4. SEM images of PdAu layer cross sections after utilization for H_2O_2 synthesis with view of (A) the M1 top surface and (B) the M2 support interface.

that homogeneous alloying of 3 μm thick PdAu layers will require significantly longer than the here applied 300 h at 823 K.

The average Au amount of membranes M1 and M2 was 13.1 and 9.5 at.%, respectively, but the Au content of the top surface should be more relevant with regard to the catalytic activity of theses membranes for H_2O_2 synthesis. Therefore the PdAu top surface was further examined by EDS and XPS, yielding Au fractions similar to those derived from XRD patterns. In particular, surface sensitive XPS indicates that Au was neither significantly depleted nor enriched in the catalytically active zone of the membranes. The XPS binding energies of the Au $4f_{7/2}$ and Au $4f_{5/2}$ states were 84.1

Table 3
Characterization of PdAu layer compositions.

Membrane	Fragments	Method	Au content (at.%)	
			Top	Bottom
M1	3	XRD	14.0 ± 0.7	12.1 ± 1.1
	3	EDS	17.5 ± 0.7	
	1	XPS	13.2	
M2	5	XRD	12.0 ± 0.9	7.0 ± 3.4
	1	EDS	12.9	
	1	XPS	7.8	

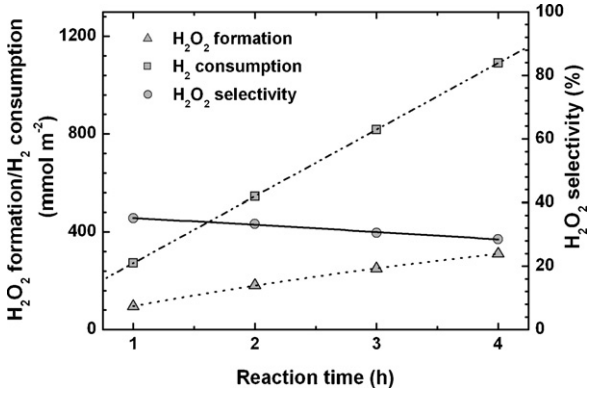

Fig. 5. H_2O_2 formation over membrane M2 as function of reaction time at 348 K and P_{res} = 300 kPa.

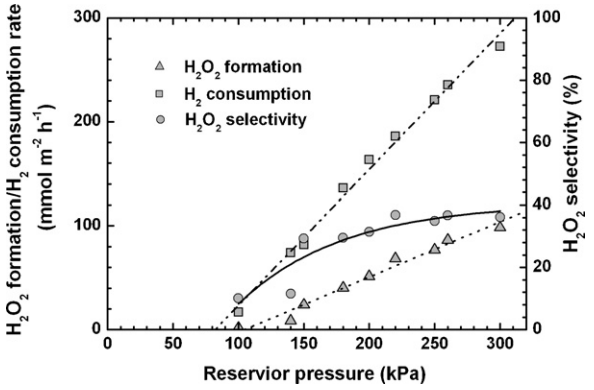

Fig. 7. Effect of H_2 reservoir pressure on H_2O_2 formation over membrane M2 at 348 K.

and 87.7 eV, respectively, which are characteristic values for metallic Au [15]. Binding energies of 335.8 and 341.3 eV of the Pd $3d_{5/2}$ and Pd $3d_{3/2}$ states were somewhat larger than those of pure Pd. This may indicate partial oxidation of Pd at the membrane surface since the $3d_{5/2}$ state of metallic Pd occurs around 335.0 eV whereas a peak at 335.6 eV has been attributed to oxygen-chemisorbed Pd [16].

3.2. H_2O_2 synthesis

Fig. 5 shows H_2O_2 yield and selectivity as well as H_2 consumption in aqueous solution as function of reaction time at 348 K and 300 kPa H_2 reservoir pressure. The H_2O_2 yield grew with time but its growth rate gradually slowed down. This is caused by a decline of the H_2O_2 selectivity from 35% to 29% since the H_2 consumption rate increased linearly from 273 mmol m^{-2} after 1 h to 1091 mmol m^{-2} after 4 h. The decrease of H_2O_2 selectivity suggests that H_2O_2 decomposition or reduction became increasingly significant.

Fig. 6 shows H_2O_2 formation rate and selectivity as well as H_2 consumption rate in aqueous reaction medium as function of temperature at P_{res} = 300 kPa. The H_2O_2 formation rate increased fivefold from 19.5 to 97.5 mmol m^{-2} h^{-1} between 277 and 363 K despite a simultaneous decline of H_2O_2 selectivity from 56% to 30%. The H_2O_2 productivity gain is obviously owed to the much faster acceleration of H_2 consumption with temperature. The activation energy derived from the H_2 consumption rates is 21.7 kJ mol^{-1}.

Fig. 7 shows H_2O_2 formation rate and selectivity together with H_2 consumption rate in aqueous solution as function of H_2 reservoir pressure at 348 K. All three quantities increased with P_{res}. The H_2 consumption rate increased linearly with P_{res}, but H_2O_2 formation accelerated faster at low H_2 reservoir pressures because of the parallel selectivity improvement, which approached a limiting value of 37% above P_{res} = 200 kPa. H_2O_2 formation was minimal, i.e. 1.7 mmol m^{-2} h^{-1}, at the lowest reservoir pressure and reached 95.8 mmol m^{-2} h^{-1} when P_{res} had reached 300 kPa.

Fig. 8 shows that H_2 consumption, H_2O_2 formation and H_2O_2 selectivity increased moderately with ethanol content at 333 K and P_{res} = 140 kPa, although H_2O_2 selectivity practically leveled off at ca. 42% in solutions with more than 40% ethanol. In ethanol the H_2O_2 formation rate reached 46.7 mmol m^{-2} h^{-1} and was ca. 10 mmol m^{-2} h^{-1} higher than in water while H_2 consumption accelerated from 98 to 112 mmol m^{-2} h^{-1} in parallel. However, when P_{res} was raised to 180 kPa in solutions with more than 50% ethanol, the color of M1 began to change from the normal metallic luster to dark grey, followed soon by partial delamination of the alloy layer. This phenomenon was repeatedly observed in ethanolic reaction media but did not occur in pure water containing 0.03 M H_2SO_4, where P_{res} could be raised up to the experimental limit 300 kPa without problem. Note that membrane M2 had been operated for more than 40 h in acidic solutions during the above described H_2O_2 synthesis experiments. The cause for the surprising instability of the PdAu layer in ethanolic solutions has not been further investigated.

4. Discussion

The differing XRD patterns of the top and interface sides demonstrate that stability of the H_2 permeation rate is not a sufficient criterion for homogeneity of alloy layers prepared from consecutively deposited Pd and Au layers. This lack of sensitivity is probably

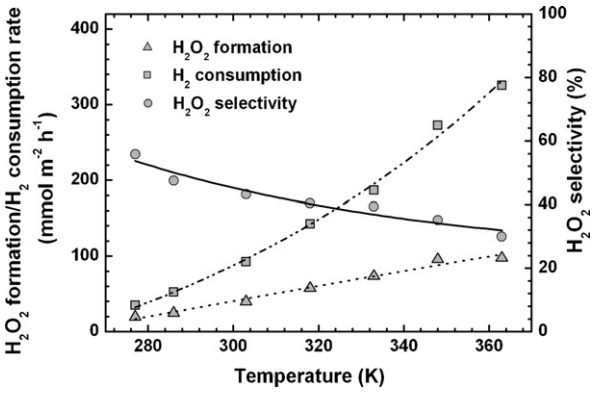

Fig. 6. Effect of temperature on H_2O_2 productivity over M2 at P_{res} = 300 kPa.

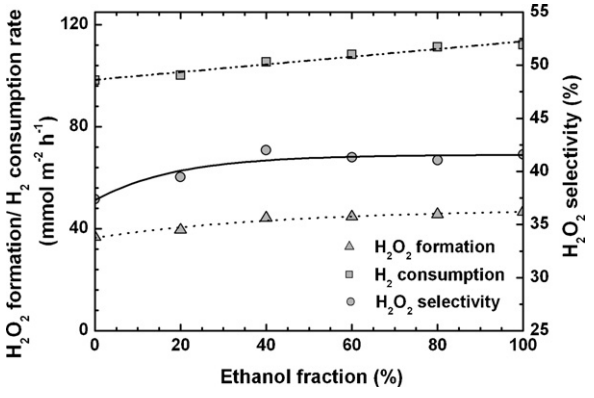

Fig. 8. H_2O_2 formation and selectivity as function of ethanol content in the reaction medium over membrane M1 at 333 K and P_{res} = 140 kPa.

owed to the weak variation of H_2 permeability of PdAu alloys with up to 15 at.% Au [10]. Conversely, the observed degree of heterogeneity has a negligible impact on the H_2 permeation rates of the here employed membranes. On the other hand, it is not clear how H_2 permeation is affected by the large voids in the PdAu layers, which are presumably caused by hydrogen [17]. Obviously the resulting spongelike morphology poses a significant obstacle to metal interdiffusion between top and bottom of the metal layer. Since homogenization of the M1 PdAu layer has much further progressed despite having much larger voids, it can be assumed that these pores did not primarily evolve during the initial annealing at 823 K but rather during subsequent operation of the membranes at lower temperatures. Nevertheless, the texture and composition of the reaction side membrane surface are of larger importance in the context of catalytic oxidation of hydrogen than its internal morphology and stoichiometry. Hence it needs to be emphasized that the voids did not reach the surface and the PdAu layers remained continuous according to SEM measurements after conclusion of all experiments (Fig. 4).

The H_2 permeability of the here prepared membranes is in the range of previously studied PdAu/ceramic composite membranes. For example, the permeability of M1 reached 6×10^{-9} mol m^{-1} s^{-1} Pa$^{-0.5}$ at 673 K, which is similar to that of a PdAu membrane with ca. 6 at.% Au prepared by Okazaki et al. on a capillary support [18]. The permeability of M2 is even twice as high and thus approaches that of 25 μm thick, unsupported PdAu foils with ca. 12 at.% Au [19]. Note that an early report by Rodina et al. indicated an even higher permeability for a metallurgically prepared $Pd_{87}Au_{13}$ foil of 0.1 mm thickness, i.e. ca. 2.7×10^{-8} mol m^{-1} s^{-1} Pa$^{-0.5}$ at 673 K [20]. Interestingly, H_2 permeation through this foil declined also much faster with decreasing temperature below 573 K [20] as observed here for the 2–3 μm thick supported membranes. Such discontinuities in the temperature dependence indicate a change of the permeation rate controlling step, typically from diffusion-limited H_2 transport at high to a desorption or adsorption-limited process at low temperatures [21,22]. The high temperature activation energy of 15.8 kJ mol^{-1} derived from tabulated H_2 fluxes for the $Pd_{87}Au_{13}$ foil [20] is higher than the values around 11 kJ mol^{-1} determined for H_2 permeation through M1 and M2 (Table 2) above 573 K, but the latter agree very well with the 11.3 kJ mol^{-1} reported for PdAu/ceramic capillary membranes [18].

H_2O_2 productivity over these PdAu membranes was considerably lower than over a Pd membrane, which we employed in a previous study. For example, 133 mmol m^{-2} h^{-1} H_2O_2 were obtained over the latter at 348 K and P_{res} = 300 kPa [7], which exceeds the formation rate over the PdAu membrane by almost 40% under identical synthesis conditions. At 303 K H_2O_2 formation was even twice as fast over the Pd membrane. The better performance of the Pd membrane catalyst at high temperature can be fully attributed to the 1.4 times higher H_2 consumption since H_2O_2 selectivity was identical (35%) over both membrane types at 348 K. At low temperatures, however, H_2O_2 selectivity was lower over the PdAu membrane (e.g. 43% vs. 59% at 303 K and P_{res} = 300 kPa), leading to the even larger performance gap between both membrane catalysts.

The lower H_2O_2 productivity over PdAu membranes is not the result of the intrinsic H_2 permeability of these membranes, which can be extrapolated from the gas permeation measurements between 423 and 523 K in the absence of liquid media on the permeate side (Table 2). For example, the accordingly estimated intrinsic H_2 permeation rate of M2 amounts to 0.0306 mol m^{-2} s^{-1} (=110,000 mmol m^{-2} h^{-1}) at 348 K and $\Delta P_{H_2} = 100$ kPa. Hence, it exceeds the H_2 consumption rates displayed in Fig. 5 by more than two orders of magnitude. Therefore, hydrogen transport within the PdAu membrane is unlikely to have a significant effect on H_2O_2 formation under the here employed conditions. This is corroborated by the activation energy for H_2 consumption during H_2O_2 synthesis (21.7 kJ mol^{-1}), which is twice as high as that for diffusion-limited hydrogen permeation derived from the measurements above 573 K (Table 2). Although the activation energy for H_2 consumption is in the range of those observed for H_2 permeation below 573 K (Table 2), it is unlikely that H_2 desorption or adsorption control the H_2 consumption rate in the liquid phase PdAu membrane reactor either.

Instead we presume that the rate of oxidative removal of hydrogen on the liquid phase reaction side membrane surface determines H_2 transfer through the PdAu membrane as we have previously argued for H_2O_2 synthesis over Pd membranes [7]. Indeed, the activation energy for H_2 consumption during H_2O_2 synthesis over the PdAu membrane is very similar to the corresponding value determined using a Pd membrane (20.3 kJ mol^{-1} [7]), and both compare well with the activation energy of 22.3 kJ mol^{-1} for H_2O_2 formation over a Pd/SiO_2 catalyst [23]. The H_2O_2 selectivity improvement with H_2 feed pressure, which occurs over PdAu as well Pd membranes, points also to their catalytic activity as the key factor for H_2O_2 productivity. This selectivity gain signals that the enhancement of the H_2O_2 formation rate with H_2 feed pressure outbalances the net effect of the latter on the direct H_2O formation and the H_2O_2 reduction rate. Since H_2O_2 reduction accelerates faster with H_2 feed pressure than H_2O_2 formation over Pd catalysts [7,23,24], it is clear that direct H_2O formation must slow down appreciably on the surface of these membranes at the same time.

The dwindling of the direct H_2O formation channel can be rationalized considering the microscopic kinetics of H_2 oxidation on Pd surfaces established in surface science and computational studies [7]. The O–O bond is not broken during formation of H_2O_2 over Pd catalysts in aqueous solution [25], whereas ultrahigh vacuum (UHV) studies show that O_2 first dissociates and forms the key intermediate OH with co-adsorbed H atoms during H_2O formation on Pd surfaces [26]. Theoretical studies indicate that O_2 dissociation and H_2O_2 formation proceed via adsorption at bridge sites on Pd surfaces [27,28]. Obviously additional adsorption sites are required in the vicinity for the emerging atomic O in the case of dissociation. However, O like H atoms adsorb preferentially at threefold coordinated hollow sites with bridge sites being the only other, very weak O adsorption site on Pd surfaces [27,29]. It is plausible that potential O adsorption sites are increasingly blocked as more and more H atoms emerge on the reaction side membrane surface with increasing H_2 feed pressure. As a consequence O_2 dissociation becomes kinetically inhibited at high H_2 feed pressure because of lacking free O adsorption sites. H_2O_2 formation on the other hand benefits from H atoms at nearby hollow sites according to a recently proposed mechanism for H_2O_2 synthesis on Pd and PdAu surfaces [28]. Note that the particularly strong increase of H_2O_2 selectivity with H_2 feed pressure at the lowest investigated temperatures can be also rationalized within the established framework of microkinetics considering the energetics of the two viable reaction channels for direct H_2O formation on Pd, i.e. hydroxyl disproportionation and addition of H atoms to hydroxyl groups [7]. Hence, surface reaction kinetics dominate H_2O_2 synthesis over both Pd and PdAu membranes and the enhancement of the H_2O_2 formation rate with temperature and H_2 feed pressure is primarily owed to a combination of accelerated reaction kinetics and suppression of direct H_2O formation and not the faster delivery of hydrogen through the membranes.

In this view it is remarkable that the efficiency of PdAu membranes for H_2O_2 synthesis is much lower than that of Pd membranes, which contrasts markedly with the reverse catalytic activity of supported Pd and PdAu powder catalysts [8]. Those nanostructured catalysts have in general much higher Au contents of at least 35 at.%. Their superior performance results to a large extent from

significantly improved H_2O_2 selectivities with respect to Pd catalysts, whereas the H_2O_2 selectivity of the PdAu membranes is comparable to that of the Pd membrane catalyst at high temperature and somewhat lower around room temperature. Thus, H_2O_2 formation kinetics appear to be slower at the PdAu membrane surface. The catalytic activity of the powder catalysts depends on a number of factors including Pd/Au stoichiometry, PdAu particle size and morphology, and nature of the support material [8]. For example, Al_2O_3 and TiO_2 supported PdAu nanocrystals exhibit a core-shell morphology with Pd segregated to the surface while homogenously alloyed catalyst particles prevail on carbon supports [8]. The optimum Pd/Au ratio also varies with the nature of the support amounting to 2 for TiO_2 and carbon but only to 0.35 for Al_2O_3. All of these catalysts exhibit significantly higher activity for H_2O_2 synthesis than pure Pd and Au catalysts on the respective support materials, with the carbon supported PdAu catalysts performing the best by far [8]. The interplay between all of these factors is not well understood yet, but it is clear that the nature of the support material plays a key role in the activity of these nanostructured catalysts.

Obviously, such support contributions are not relevant if dense membranes are used as here. Instead, the catalytic activity of PdAu membrane catalysts is likely governed by the alloy composition at their surface. In general, the lower surface energy of Au favors segregation of Au to PdAu alloy surfaces with Pd atoms interspersed, and it has been proposed that such isolated Pd monomers on Au surfaces are responsible for the enhanced acetoxylation of ethylene to vinylacetate on PdAu catalysts [30]. However, XPS results indicate that neither Au nor Pd are significantly enriched on the surface of the here used PdAu membranes so that promotion of H_2O_2 formation through monomeric Pd cannot be expected in the present study. Still, it is conceivable that the surface Au concentration of these membranes is a critical parameter for their catalytic activity, which should be elucidated in further studies.

Addition of moderate amounts of ethanol to the reaction medium has evidently a positive effect on the H_2O_2 formation rate and in particular H_2O_2 selectivity. This can be attributed to the higher solubility of O_2 in the solution since H_2 is apparently quantitatively consumed at the membrane surface before it can desorb into the solution. Therefore it is expected that H_2O_2 productivity can be significantly improved at elevated O_2 feed pressures as previously shown for direct H_2O_2 synthesis in a membrane contactor [4].

5. Conclusions

Thin layered PdAu membranes have been prepared by electroless plating of Pd and Au on porous ceramic tubes. Alloying of the metal layers was incomplete after more than 250 h annealing despite that the H_2 permeation rates had stabilized after that time. Still, the H_2 permeability of the membrane with a 3 μm thick $Pd_{90.5}Au_{9.5}$ layer reached 1.2×10^{-8} mol m^{-1} s^{-1} Pa$^{-0.5}$ at 673 K, which is among the highest values reported for supported PdAu membranes so far. Investigation of the temperature dependence revealed two distinct H_2 permeation regimes. Above 573 K it was controlled by hydrogen diffusion through the bulk of the PdAu layers while surface processes likely became transport rate limiting below that threshold. H_2 permeation was drastically further reduced when the membranes were immersed in acidic water/ethanol mixtures for study of direct H_2O_2 synthesis from H_2 and O_2 as evidenced by the H_2 consumption rates. These were orders of magnitude smaller than the intrinsic H_2 permeation rates at the corresponding temperatures, which were extrapolated from the permeation measurements in the absence of the liquid reaction media.

In contrast to PdAu powder catalysts, which exhibit significantly higher activity for H_2O_2 synthesis than analogous Pd powder catalyst, H_2O_2 productivity was noticeably lower over the PdAu membranes in comparison to a Pd membrane. H_2O_2 selectivity of the PdAu membranes was similar to that of the Pd membrane at the highest temperatures, but did not increase as much with decreasing reaction temperature as it did in the case of the Pd membrane. H_2O_2 formation and H_2 consumption rates increased significantly with temperature on the other hand but fell always short of the values observed using the Pd membrane. The enhancement of H_2O_2 selectivity with H_2 feed pressure is credited to inhibition of direct H_2O formation as a result of hindered O_2 dissociation due to blocking of O atom adsorption sites on the membrane surface because of increasing occupation by H atoms. Furthermore, H_2O_2 selectivity and formation rate increased moderately with ethanol content at 333 K due to larger O_2 solubility in the solution. However the PdAu layers tended to delaminate if the ethanol concentration was raised above 50%, so that it needs to be kept below that limit with the presently used membranes.

Acknowledgement

We gratefully acknowledge financial support from the Ministry of Science and Technology of China (Grant No. 2005CB221401).

References

[1] J.M. Campos-Martin, G. Blanco-Brieva, J.L.G. Fierro, Angew. Chem. Int. Ed. 45 (2006) 6962.
[2] V.R. Choudhary, A.G. Gaikwad, S.D. Sansare, Angew. Chem. Int. Ed. 40 (2001) 1776.
[3] S. Abate, S. Melada, G. Centi, S. Perathoner, F. Pinna, G. Strukul, Catal. Today 117 (2006) 193.
[4] A. Pashkova, K. Svajda, R. Dittmeyer, Chem. Eng. J. 139 (2008) 165.
[5] R. Noyori, M. Aoki, K. Sato, Chem. Commun. (2003) 1977.
[6] W.G. Cheng, X.S. Wang, G. Li, X.W. Guo, S.J. Zhang, J. Catal. 255 (2008) 343.
[7] L. Shi, A. Goldbach, G.F. Zeng, H.Y. Xu, J. Membr. Sci. 348 (2010) 160.
[8] J.K. Edwards, A.F. Carley, A.A. Herzing, C.J. Kiely, G.J. Hutchings, Faraday Discuss. 138 (2008) 225.
[9] A. Maeland, T.B. Flanagan, J. Phys. Chem. 69 (1965) 3575.
[10] J. Shu, B.P.A. Grandjean, A. Van Neste, S. Kaliaguine, Can. J. Chem. Eng. 69 (1991) 1036.
[11] G.F. Zeng, A. Goldbach, H.Y. Xu, J. Membr. Sci. 326 (2009) 681.
[12] L. Shi, A. Goldbach, G.F. Zeng, H.Y. Xu, Int. J. Hydrogen Energy 35 (2010) 4201.
[13] R.J.R. Uhlhorn, K. Keizer, A.J. Burggraaf, J. Membr. Sci. 46 (1989) 225.
[14] A. Maeland, T.B. Flanagan, Can. J. Phys. 42 (1964) 2364.
[15] J.L. Rousset, F.J. Cadete Santos Aires, B.R. Sekhar, P. Mélinon, B. Prevel, M. Pellarin, J. Phys. Chem. B 104 (2000) 5430.
[16] K.S. Kim, A.F. Grossmann, N. Winograd, Anal. Chem. 46 (1974) 197.
[17] J. Galuszka, R.N. Pandey, S. Ahmed, Catal. Today 46 (1989) 83.
[18] J. Okazaki, D.A. Pacheco Tanaka, M.A. Llosa Tanco, Y. Wakui, T. Ikeda, F. Mizukami, T.M. Suzuki, Mater. Trans. 49 (2008) 449.
[19] D.L. McKinley, US Patent 3,350,845 (1967).
[20] A.A. Rodina, M.A. Gurevich, V.A. Stroeva, N.I. Doronicheva, Russ. J. Phy. Chem. 40 (1966) 1104.
[21] T.L. Ward, T. Dao, J. Membr. Sci. 153 (1999) 211.
[22] L.X. Yuan, A. Goldbach, H.Y. Xu, J. Phys. Chem. B 111 (2007) 10952.
[23] Y. Voloshin, R. Halder, A. Lawal, Catal. Today 125 (2007) 40.
[24] Y. Voloshin, A. Lawal, Appl. Catal. A 353 (2008) 9.
[25] D.P. Dissanayake, J.H. Lunsford, J. Catal. 214 (2003) 113.
[26] C. Nyberg, C.G. Tengstål, J. Chem. Phys. 80 (1984) 3463.
[27] K. Honkala, K. Laasonen, J. Chem. Phys. 115 (2001) 2297.
[28] A. Staykov, T. Kamachi, T. Ishihara, K. Yoshizawa, J. Phys. Chem. C 112 (2008) 19501.
[29] W. Dong, G. Kresse, J. Furthmüller, J. Hafner, Phys. Rev. B 54 (1996) 2157.
[30] M.S. Chen, D. Kumar, C.-W. Yi, D.W. Goodman, Science 310 (2005) 291.